

## Neutral-ionic phase transition of (BEDT-TTF)(ClMeTCNQ) under pressure

T. Hasegawa,<sup>1</sup> T. Akutagawa,<sup>1</sup> T. Nakamura,<sup>1</sup> T. Mochida,<sup>2</sup> R. Kondo,<sup>3</sup> S. Kagoshima,<sup>3</sup> and Y. Iwasa<sup>4</sup>

<sup>1</sup>Research Institute for Electronic Science, Hokkaido University, Sapporo 060-0812, Japan

<sup>2</sup>Department of Chemistry, Toho University, Funabashi 274-8510, Japan

<sup>3</sup>Department of Basic Science, The University of Tokyo, Komaba, Tokyo 153-8902, Japan

<sup>4</sup>Japan Advanced Institute of Science and Technology (JAIST), Ishikawa 923-1292, Japan

(Received 26 October 2000; revised manuscript received 26 March 2001; published 7 August 2001)

Observation and characterization are reported on a neutral-ionic (NI) phase transition under pressure in (BEDT-TTF)(ClMeTCNQ), which is a mixed-stack charge-transfer compound with BEDT-TTF-based intercolumnar networks. Optical and electrical experiments revealed that the compound undergoes a pressure-induced NI transition at 1 GPa at room temperature. The temperature-pressure phase diagram of this phase transition was established by the electrical resistivity measurements at low temperature under pressure. The observed symmetry breaking in the infrared spectra and dramatic decrease of resistivity indicate that the NI transition in (BEDT-TTF)(ClMeTCNQ) at 1 GPa at room temperature is qualitatively similar in nature to that in the standard material (TTF)(CA). In contrast, the NI transition in (BEDT-TTF)(ClMeTCNQ) at low temperature under lower pressure considerably differs from that in (TTF)(CA) as to the resistivity behaviors around the phase boundary: The former becomes almost continuous without showing any anomaly, while the latter is significantly discontinuous. We discuss the origin of the observed electrical behaviors in (BEDT-TTF)(ClMeTCNQ) in terms of the effect of intercolumnar interaction associated with BEDT-TTF moieties.

DOI: 10.1103/PhysRevB.64.085106

PACS number(s): 71.30.+h, 72.80.Le, 78.30.Jw, 78.40.Me

### I. INTRODUCTION

The electron donor molecule BEDT-TTF [bis(ethylene-dithio)tetrathiafulvalene] and its analogs afford plenty of organic metals and superconductors by forming charge-transfer (CT) salts with inorganic counter anions.<sup>1</sup> This stable metallicity is derived from the *side-by-side* interaction between BEDT-TTF cations.<sup>2,3</sup> In contrast, understanding of the donor-acceptor- (*DA*-) type CT complexes of BEDT-TTF with organic acceptor (*A*) molecules remains extremely poor. However, from recent investigation of (BEDT-TTF)(TCNQ)-type compounds (TCNQ=tetracyanoquinodimethane),<sup>4-9</sup> combinations of the BEDT-TTF analogs with kinds of electron acceptors of TCNQ-halogenated derivatives are found to afford a rich variety of two-component CT complexes, including the first *DA*-type superconducting complex.<sup>8</sup> The following unique features are observed in the (BEDT-TTF)(TCNQ) systems, which are in sharp contrast to the conventional *DA*-type two-component systems: (1) Construction of a variety of crystal structures, due to the complex formation of BEDT-TTF's, having two-dimensional (2D) nature in the intermolecular interactions, with TCNQ's, which exhibit highly anisotropic interactions. (2) Suppression of Peierls (or spin-Peierls) instability in spite of the existence of TCNQ columns. (3) Strongly localized nature of TCNQ anion radicals in their crystal lattices, which contribute to the magnetic properties of these complexes.

Among the (BEDT-TTF)(TCNQ) systems, CT complexes composed of 1:1 mixed stacks of *D* and *A* molecules are most promising to afford peculiar electronic properties to such *DA*-type systems, since the direct CT interaction between *D* and *A* molecules dominates over their electronic properties. In an isomorphous series of such mixed-stack (BEDT-TTF)(TCNQ) systems, the effects of the introduction of BEDT-TTF analogs are prominent, where the *side-by-side*

intercolumnar overlaps become comparable to the *face-to-face* overlaps between the *D* and *A* molecules along the mixed stacks, as is confirmed by the extended Hückel intermolecular overlap calculations.<sup>9</sup> Actually, the ionic compound of (BEDO-TTF)(Cl<sub>2</sub>TCNQ) has been found to be a magnetic insulator and preserves the regular mixed-stack structure down to low temperature. The drastic magnetic phase transition was observed in this compound with maintaining their regular stacks, which forms a marked contrast to the conventional "dimerized" mixed-stack nonmagnetic ionic compounds.<sup>9</sup>

These unique features of the mixed-stack (BEDT-TTF)(TCNQ) systems should provide an opportunity to explore aspects of the neutral-ionic (NI) phase transition, which is a well-known unique phenomenon of the mixed-stack compounds.<sup>10</sup> The lattice contraction, caused by application of pressure or reduction of temperature, induces a phase transition from the neutral (small degrees of CT) to the ionic (large degree of CT) states, via an increase of the Madelung energy.<sup>11</sup> To date, research into the NI phase transitions has been limited to those which have a strong one-dimensional nature along the *DA* stacks.<sup>10,12,13</sup> For example in (TTF)(CA) (TTF=tetrathiafulvalene, CA=chloranil), the change of the molecular valence is accompanied by the simultaneous stack dimerization in the ionic *DA* stacks.<sup>14-16</sup> By contrast, the effect of the strong intercolumnar interaction by BEDT-TTF's is expected to suppress the 1D instability to lattice dimerizations in the ionic phases, as is observed in the ionic state of (BEDO-TTF)(Cl<sub>2</sub>TCNQ), which is free from dimerization. Thus, in principle, we can anticipate an occurrence of NI phase transitions without associating dimerizations. In such a case, the transition becomes purely electronic, and various unconventional electronic properties should be found: high electrical conductivity at the NI border, the magnetic NI transition, or new quantum aspects.

For these purposes, we have chosen (BEDT-TTF)(ClMeTCNQ) among an isomorphous series of the mixed-stack systems. This complex is located closest to the NI border, considering the observed CT excitation energy in the optical spectra,<sup>10</sup> though they keep neutral states down to low temperature at ambient pressure. In this paper, we report the observation and characterization of the NI phase transitions in (BEDT-TTF)(ClMeTCNQ) under pressure. The nature of the room-temperature NI phase transition was investigated by optical spectra as well as by the resistivity measurement. Also, the temperature-pressure phase diagram was established by measurements on the temperature dependence of the electrical resistivity. These experimental results revealed that (1) the NI transition at 1 GPa at room temperature in (BEDT-TTF)(ClMeTCNQ) is quite similar to that in the standard material (TTF)(CA) and (2) the low-temperature and lower-pressure NI transition becomes more and more continuous with decreasing the transition temperature, in marked contrast to the case of (TTF)(CA), where discontinuity becomes prominent at low temperature. In principle, the NI transition is derived by the Madelung interaction, but in the real transition in 1D mixed-stack CT compounds like (TTF)(CA), the dimerization instability<sup>17,18</sup> and the concomitant quasi-one-dimensional (Q1D) ferroelectric fluctuation play crucial roles in the discontinuity of the NI transition. Taking this understanding of the conventional NI transition into account, the continuous NI transition in (BEDT-TTF)(ClMeTCNQ) may be ascribed to a suppression of a ferroelectric fluctuation and/or a reduction of the degree of the dimerization, which are rationalized by the introduction of the intercolumnar interaction of BEDT-TTF molecules.

## II. EXPERIMENT

The compound (BEDT-TTF)(ClMeTCNQ) was synthesized following the previous paper.<sup>9</sup> The maximum size of the single crystals reached about 1.6 mm×1.7 mm×13 mm.

The optical absorption spectra at high pressure to 4.0 GPa were measured using a diamond anvil cell for powdered samples dispersed in pressure medium poly(chloro trifluoro) ethylene oil (Merck). The absorption spectra were recorded on a grating (JASCO CT-25) and a Fourier transform infrared (FTIR) spectrometer (Nicolet Magna 900) for the UV-visible and infrared regions, respectively. The applied pressure was monitored by the photoluminescence of ruby excited by an Ar-ion laser (514.5 nm).

The measurements of electrical resistivity were made with use of a clamp-type high-pressure cell. The hydrostatic pressure was produced with a pressure medium Daphne 7373 (Idemitsu).<sup>19</sup> The resistance was measured both by four-probe and two-probe methods, simultaneously, for a temperature range of 4.2–300 K at various pressures ranged over 0.3–1.8 GPa.

## III. RESULTS

### A. Optical spectra under pressure

The intramolecular electronic excitations were observed in the near-infrared and visible range for (BEDT-

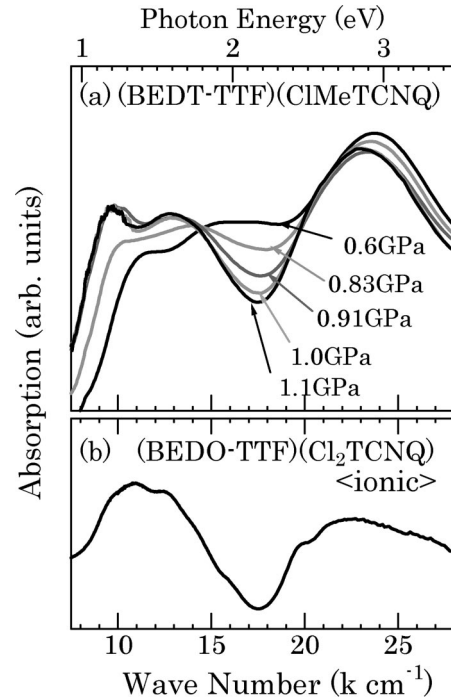


FIG. 1. (a) Intramolecular electronic excitation spectra of (BEDT-TTF)(ClMeTCNQ) in the near-infrared to visible range under various pressures at room temperature. Large variations of the spectra are observed around 0.6–1.1 GPa. (b) Electronic spectrum of an isomorphous ionic compound of (BEDO-TTF)(Cl<sub>2</sub>TCNQ) is shown for comparison.

TTF)(ClMeTCNQ). At ambient pressure, the spectra exhibited three major features peaking at around 11 500, 16 000, and 24 000 cm<sup>-1</sup>, respectively. In Fig. 1(a), we plotted the absorption spectra of (BEDT-TTF)(ClMeTCNQ) measured at various pressures. The spectra exhibited appreciable variations with applying pressure in the range 0.6–1.1 GPa; the appearance of new features was detected at around 9 500 cm<sup>-1</sup> and 13 000 cm<sup>-1</sup>, which increased their intensities gradually with the application of pressure, while the peaks around 11 500 cm<sup>-1</sup> and 16 000 cm<sup>-1</sup> disappeared. The largest feature observed at around 24 000 cm<sup>-1</sup> slightly shifted to a lower energy of about 600 cm<sup>-1</sup>. Further spectral change was not observed at pressure higher than 1.1 GPa.

In Fig. 1(b), we show the absorption spectrum of (BEDO-TTF)(Cl<sub>2</sub>TCNQ), which is isomorphous but has an ionic ground state at ambient pressure.<sup>9</sup> As seen in the comparison of these spectra, the whole spectral features of (BEDT-TTF)(ClMeTCNQ) at 1.1 GPa are almost identical with those of (BEDO-TTF)(Cl<sub>2</sub>TCNQ), providing clear evidence that the pressure-induced spectral change of (BEDT-TTF)(ClMeTCNQ) is ascribed to the valence change from the neutral to the ionic states. Among these features, the absorption bands observed at around 9 000–14 000 cm<sup>-1</sup> were attributed to the transitions from the second highest occupied molecular orbital (HOMO-1) to the HOMO of BEDT-TTF molecules. The intensity of these bands is known to be strongly dependent on the valence of BEDT-TTF molecules.<sup>6</sup> The observed slight redshift of the 25 000 cm<sup>-1</sup> peak which

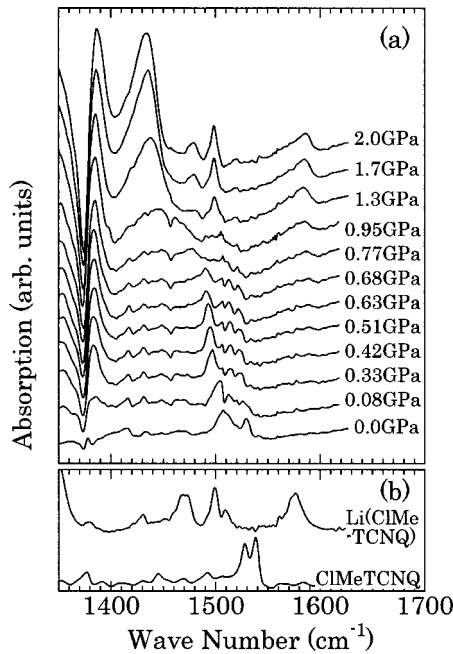


FIG. 2. (a) Intramolecular vibrational spectra of (BEDT-TTF)(CIME TCNQ) under various pressures at room temperature. (b) Vibrational spectra of Li(CIME TCNQ) and neutral CIME TCNQ at ambient pressure are shown for comparison.

was attributed to the excitation from the HOMO to the lowest unoccupied molecular orbital (LUMO) excitation of donors and acceptors is also consistent with the neutral-ionic phase change.<sup>10</sup>

In Fig. 2(a), we show the infrared vibrational spectra of (BEDT-TTF)(CIME TCNQ) at various pressures. The vibrational spectra for C=C double bonds exhibited noticeable variations with application of pressure, providing evidence of the NI phase transition; the feature at about  $1510\text{ cm}^{-1}$ , which is ascribed to the CIME TCNQ intramolecular C=C vibrations, gradually lowered the peak energy with applying pressure down to about  $1490\text{ cm}^{-1}$  below 0.8 GPa. This feature indicates the gradual variation of the degree of CT with the application of pressure. In contrast, in the ionic states above 1.2 GPa, the C=C vibrations stayed at about  $1480$  and  $1500\text{ cm}^{-1}$ , which roughly correspond to the almost complete CT ( $\rho \sim 1$ ), from comparison with the vibrational spectra of Li(CIME TCNQ) shown in Fig. 2(b). In the vicinity of the NI transition, these features undergo appreciable broadening, as seen in the spectra at 0.77 GPa and at 0.95 GPa.

The pressure-induced change is even more remarkable in the broad and intense feature at around  $1430\text{ cm}^{-1}$ , which gradually appears when the pressure was raised to about 0.9–1.0 GPa. This band can be attributed to a sign of the totally symmetric  $a_g$  mode of the central and ring C=C bonds in BEDT-TTF molecules.<sup>20</sup> This mode became IR active definitely above 1.2 GPa, most probably due to dimeric lattice distortions, via electron-molecular-vibration (EMV) interactions.<sup>21</sup> We also detected the  $a_g$  mode of CIME TCNQ at around  $1585\text{ cm}^{-1}$  clearly at high pressure, as seen in Fig. 2(a). A similar feature has been also observed at the NI

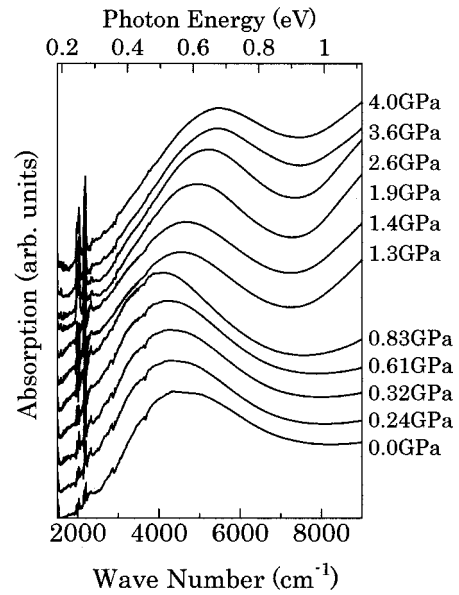


FIG. 3. Charge-transfer electronic excitation spectra of (BEDT-TTF)(CIME TCNQ) under various pressures at room temperature.

phase transition of other mixed-stack compounds.<sup>14,15,22</sup> This result indicates that the NI phase transition of (BEDT-TTF)(CIME TCNQ) is associated with the dimerization at the NI transition point of  $T = 295\text{ K}$  and  $P = 1.0\text{ GPa}$ , which will be further discussed in Sec. IV.

Figure 3 shows the CT band of (BEDT-TTF)(CIME TCNQ), observed around  $3000\text{--}5000\text{ cm}^{-1}$ , at various pressures. As seen in Fig. 3, the CT energy decreases with the application of pressure below 1.0 GPa, followed by an upturn above the pressure. The minimum of the CT energy is about  $4000\text{ cm}^{-1}$  at 1.0 GPa. Such large shift of the CT band energy has not been observed around the temperature- or pressure-induced NI phase transition of (TTF)(CA).<sup>15,23</sup> These different features for both complexes may indicate that the pressure effect is much more prominent on the increase of the transfer integral in (BEDT-TTF)(CIME TCNQ). This is consistent with the gradual increase of the CT degree, as observed in the vibrational spectra.

All the spectroscopic results of the pressure-induced NI transition are summarized in Fig. 4. We plotted the pressure dependence of (a) the vibrational bands and (b) the CT energy against pressure, respectively. We also show the pressure dependence of electrical resistivity in Fig. 4 (b) by open squares for the later discussions. As clearly evidenced from these figures, the CT degree exhibits considerable variation in the neutral states, before reaching  $\rho \sim 1$  just below the NI phase transition point. Considering the almost linear relationship between the vibrational frequency and the CT degree  $\rho$ ,<sup>24</sup> the change of the  $\rho$  value in neutral states is almost linear against pressure, in contrast to (TTF)(CA).<sup>25</sup>

### B. Pressure and temperature dependence of the electrical resistivity

(BEDT-TTF)(CIME TCNQ) exhibited a relatively high electrical resistivity of about  $10^4\text{ }\Omega\text{ cm}$  at ambient pressure

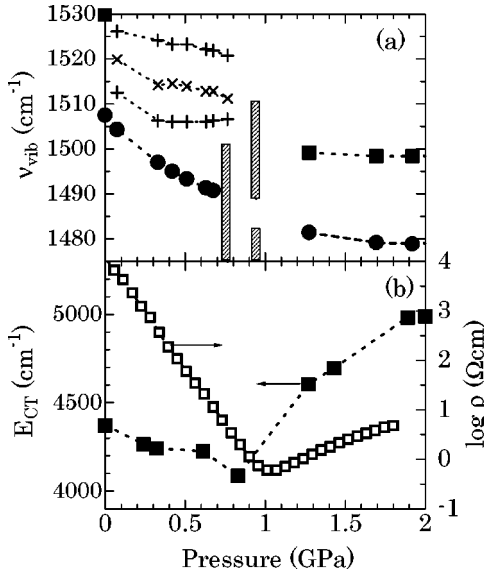


FIG. 4. (a) Pressure dependence of vibrational frequencies ( $\nu_{vib}$ ) of (BEDT-TTF)(ClMeTCNQ) around 1480–1530  $\text{cm}^{-1}$  at room temperature. Observed peak wave numbers are shown by solid squares, solid circles, and crosses. These features undergo considerable broadening in the vicinity of the NI phase boundary, as shown by the dashed areas. (b) Pressure dependence of the charge-transfer excitation energy ( $E_{CT}$ , solid squares) and electrical resistivity ( $\rho$ , open squares) of (BEDT-TTF)(ClMeTCNQ) at room temperature.

and room temperature. The resistivity was found to decrease dramatically by the application of pressure, as shown in Fig. 4(b) by open squares. The resistivity at 1.0 GPa became as low as 0.5  $\Omega \text{ cm}$  at room temperature, which was four orders of magnitude smaller than that at ambient pressure. Above a pressure of about 1.0 GPa, the resistivity started to increase against pressure. Considering the pressure-induced spectral change at around 1.0 GPa as described in the former section, this turning point should correspond to the NI phase transitions. The considerably sensitive nature of the resistivity to the applied pressure has been also observed in (TTF)(CA).<sup>26</sup>

In Fig. 5, we show the temperature dependence of electrical resistivity at various pressures, where the resistivity was plotted in a logarithmic scale against the reciprocal of the temperature (Arrhenius plot). The resistivity exhibits semi-conducting behaviors in the whole measured range. In the respective curves, we can observe distinct anomalies, shown by arrows for the curves at 0.44–0.88 GPa, which indicate the occurrence of the NI phase transitions. At 1.0 GPa, a similar inflection point is detected around  $T=290$  K, being consistent with the spectroscopic data. As seen from these plots, the NI transition temperature strongly depends on the applied pressure. The resistivity ( $\rho$ ) curves in each phase seem to be almost linear ( $\ln \rho \propto E_a/k_B T$ ,  $E_a$  = activation energy), except for the additional anomalies due to the thermal contraction of the pressure medium,<sup>27</sup> indicating that the activation energy is almost constant over a wide temperature range. The NI transitions are observed as clear variations of the activation energy from high (ionic states) to low (neutral

states), though such a variation becomes more and more obscure as the pressure decreases down to 0.44 GPa.

The pressure-temperature phase diagram derived from the resistivity experiments is given in Fig. 6. In the diagram, the neutral phase is located at the upper left side, while the lower right side of the diagram corresponds to the ionic states. The NI phase boundary approaches the low-temperature limit at about 0.3–0.4 GPa, although the boundary becomes less and less clear at low temperature. In this sense it is difficult by the electrical resistivity measurements to determine the quantum critical point ( $T=0$  K) of this NI phase transition.

The most interesting feature is that the activation energy of the ionic states depends strongly on the applied pressure in the range of 0.44–0.95 GPa, while that of the neutral states is almost independent of pressure. To show this more clearly, we plotted the activation energies against both temperature and pressure in Fig. 7. At pressure higher than 0.8 GPa, the activation energy of the ionic states is estimated to be 2300  $\text{cm}^{-1}$ , which is much larger than that of the neutral states ( $\leq 530$   $\text{cm}^{-1}$ ). However, the jump of the activation energy at the NI transition points decreases with lowering of the pressure. The activation energy of the ionic states finally becomes almost identical with that of the neutral states at around 0.4 GPa, being less than 700  $\text{cm}^{-1}$ , which makes the phase boundary obscure in this region. These results clearly indicate that the nature of the ionic states undergoes drastic changes in the pressure range of 0.4–0.8 GPa. On the basis of these experimental results, we will discuss in the next section the unique features of NI phase transitions in (BEDT-TTF)(ClMeTCNQ).

#### IV. DISCUSSION

In this section we discuss the unique aspects of the NI phase transition in (BEDT-TTF)(ClMeTCNQ) on the basis of the results of the above optical and electrical experiments. Here we focus our attention on the unique electrical features in the vicinity of the NI phase boundaries, as investigated by comparing with those of (TTF)(CA). Before going into the discussion, we mention that the observed activation energies both for neutral and ionic states (500–2300  $\text{cm}^{-1}$ ) are much smaller than the CT excitation energy (4000–5000  $\text{cm}^{-1}$ ), as in the case of (TTF)(CA).<sup>27</sup> The observed small activation energies strongly support the domain wall picture that has been previously proposed for the electrical transport in this kind of complexes;<sup>28</sup> the domain boundaries between the almost “degenerate” neutral and ionic ground states have much lower excitation energy and are responsible for the charged carriers in such systems.

At the high- $P$  and high- $T$  phase boundary of the phase diagram shown in Fig. 6, the activation energy of the ionic states is much larger than that of the neutral states, as seen in Fig. 7. As described in Sec. III A, the NI phase transition in this region accompanies the dimerizations, while the ionicity jump is considerably small at this transition point. We conjecture that the motions of the charged carriers are strongly affected mainly by the dimeric lattice distortions in the ionic lattices, which afford a considerable difference of the activation energy between the neutral and the ionic states at this

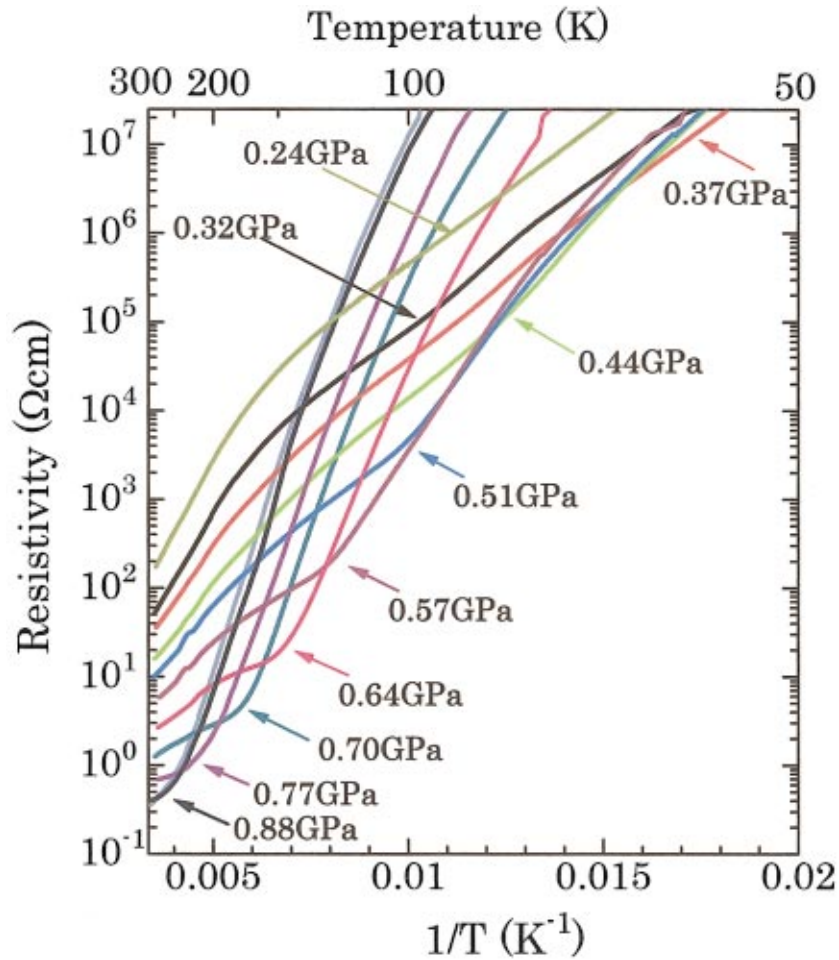


FIG. 5. (Color) Temperature dependence of the electrical resistivity of (BEDT-TTF)(ClMeTCNQ) single crystals under various pressures. The resistivity is plotted in a logarithmic scale against the reciprocal of the temperature. The neutral-ionic transitions are observed for respective curves by inflection points indicated by arrows. The pressure values are calibrated at the neutral-ionic transition temperatures for each curve.

regions. It is noted that such observed features are almost analogous to (TTF)(CA) at the phase boundary under high pressure; according to recent structural and NQR measurements,<sup>29</sup> the jump of the CT degree approaches zero at a transition point under high pressure, though the dimerizations are clearly observed.<sup>16</sup> At this transition point, the electrical resistivity of (TTF)(CA) exhibits similar anomalous

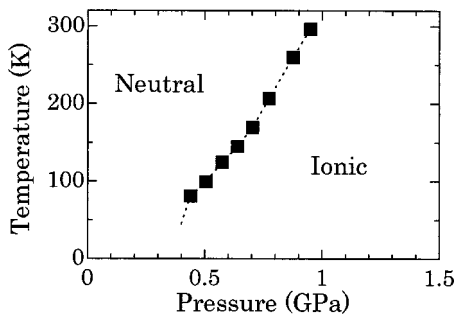


FIG. 6. Pressure-temperature phase diagram of (BEDT-TTF)(ClMeTCNQ) derived from the electrical resistivity measurements.

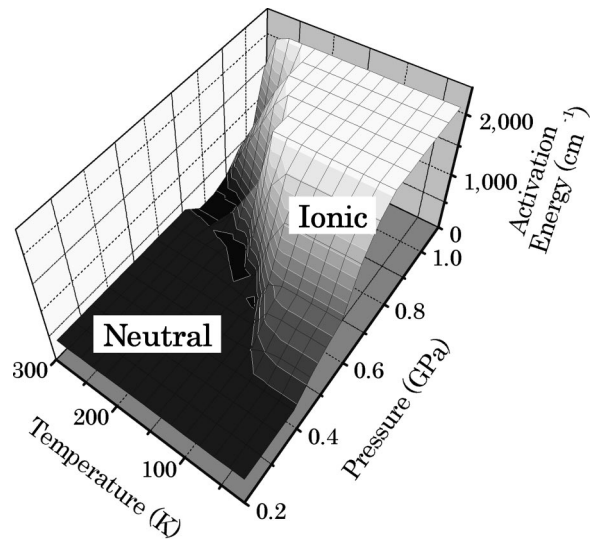


FIG. 7. Three-dimensional plot of activation energy for electrical conductivity in (BEDT-TTF)(ClMeTCNQ) against pressure and temperature.

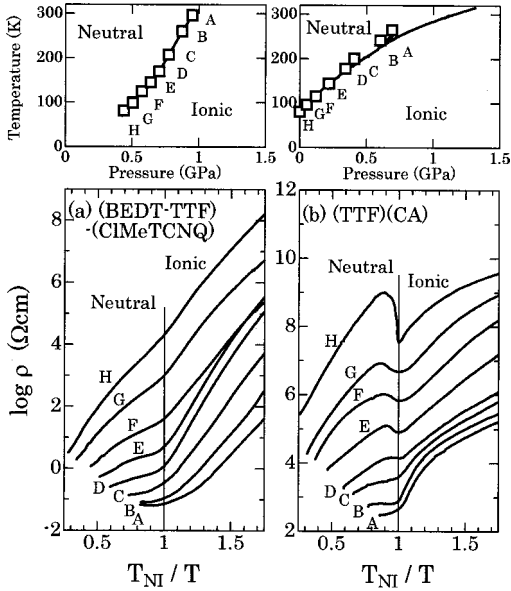


FIG. 8. Comparison of electrical behaviors of (BEDT-TTF)(CIME TCNQ) and (TTF)(CA) around neutral-ionic phase boundaries. Logarithms of the electrical resistivity are plotted against  $T_{NI}/T$  (normalized  $1/T$ ), where  $T_{NI}$  is the neutral-ionic transition temperature. Transition points for each curves are presented by open squares in the pressure-temperature phase diagrams shown in the upper figure. All the data for (TTF)(CA) are reproduced from the literatures (Refs. 27, 29, and 30).

lies, as that of (BEDT-TTF)(CIME TCNQ) at the high- $P$  and high- $T$  phase boundary.

To show this more clearly, we plotted in Fig. 8 the behaviors around the phase boundaries for (a) (BEDT-TTF)(CIME TCNQ) and (b) (TTF)(CA) (Refs. 27 and 29); logarithms of the electrical resistivity were plotted against the reciprocal temperature which is normalized by the NI transition temperature ( $T_{NI}$ ). In the respective figures, the curves located at the higher-resistivity sides are those measured at lower pressures. (See the notation A–H.) As can be seen in this figure, the curves measured at higher pressures are similar for (BEDT-TTF)(CIME TCNQ) and (TTF)(CA).

At the low- $P$  and low- $T$  phase boundaries, however, the difference of the electrical behaviors between these complexes becomes remarkable. As clearly seen from this figure, the resistivity anomaly gradually disappears at the low- $P$  and low- $T$  limit in (BEDT-TTF)(CIME TCNQ), and the transition seems to become almost continuous. In sharp contrast, the resistivity of (TTF)(CA) shows a sharp dip around the transition temperature as the applied pressure decreases. Such a clear contrast should reflect the different nature of the NI phase transitions for these complexes.

Here we should comment on the origin of the observed sharp dip in (TTF)(CA) shown in Fig. 8(b). The NI transition of (TTF)(CA) at ambient pressure is known to accompany the relatively large ( $\Delta\rho \sim 0.5$ ) ionicity jump<sup>15</sup> and the ferroelectric dipole arrangement of  $D^+A^-$  pairs over the whole crystal.<sup>16</sup> It indicates that the domain boundaries of the three possible almost degenerate phases (N and IA, IB, which are two possible orientations of the polarizations) are responsible

for the observed sharp dip in the electrical resistivity in these regions.<sup>28</sup> In particular, the thermal fluctuations of the ferroelectric arrangement of IA and IB phases have to be important, which is consistent with the results of the dielectric experiments.<sup>31,32</sup>

To explain the gradual disappearance of the resistivity anomaly in the NI phase boundary of (BEDT-TTF)(CIME TCNQ) in the low- $P$  and low- $T$  limit, which implies the almost coincidence of the activation energy of the ionic state with that of the neutral state as discussed in Sec. III B, we conjecture that the role of the intercolumnar interaction becomes responsible in the ionic states. As one of the possible scenarios for this observation, we suggest that the degree of the lattice dimerization gradually reduces with approaching the low- $P$  and low- $T$  limit of the phase boundary; in consideration of the symmetric relationship of the charged carriers between the neutral and the ionic states, it is natural to consider that the creations or motions of the ionic domains in the neutral lattices have the same activation energy with those of the neutral domains in the ionic lattices if both of these ground states have regular stacks. If the ionic lattices include the dimeric lattice distortions, such a symmetric relationship does not hold, as we described above. As denoted in Sec. III A, the further application of pressure considerably increases the transfer integral between donors and acceptors in (BEDT-TTF)(CIME TCNQ), which may increase the one-dimensional nature, to give the dimeric lattice distortions at the high- $P$  and high- $T$  NI phase boundary. In addition, we notice the difference in the temperature-pressure phase diagram in (TTF)(CA) and (BEDT-TTF)(CIME TCNQ): that the slope of the phase boundaries is rather steeper in (BEDT-TTF)(CIME TCNQ) than in (TTF)(CA). It may be also associated with a decrease in the dimerization stabilization in the low- $P$  and low- $T$  NI phase boundary of (BEDT-TTF)(CIME TCNQ).

We also admit that all of the presented experimental results may be possibly explained by another picture which does not assume any appreciable changes in the degree of the dimerizations: An intercolumnar interaction should suppress the Q1D intracolumnar fluctuations of the ferroelectric arrangement of  $D^+A^-$  dimers, which is effective in suppressing the resistivity dip around the phase boundary. We can also consider that the gradual variation of the activation energy in the ionic states is associated with the change of the charge-transfer degree ( $\rho$ ) or the change of the carrier mobility. In these meanings, further experimental and theoretical investigation on (BEDT-TTF)(CIME TCNQ) is important to elucidate the microscopic mechanism of the electrical transport around the neutral-ionic phase boundary of organic semiconductors. In particular, the detailed crystal structure analyses and measurements of the magnetic properties in low- $P$  and low- $T$  phase boundaries will be the next step for these purposes.

## V. CONCLUSIONS

In conclusion, we have found the neutral-ionic phase transition under high pressure in (BEDT-TTF)(CIME TCNQ), which is a mixed-stack charge-transfer compound with

donor-based intercolumnar networks. The NI phase boundaries were successfully determined in the temperature-pressure phase diagram for this compound on the basis of observed resistivity anomalies in the electrical measurements. In marked contrast to (TTF)(CA), we observed a gradual disappearance of the resistivity anomaly with approaching the low-temperature limit of the NI phase boundary. We suggested that a suppression of the ferroelectric fluctuation and/or a gradual reduction of the degree of the

dimerization may be associated with these experimental observations, which are rationalized by the introduction of the intercolumnar interaction of BEDT-TTF molecules.

#### ACKNOWLEDGMENT

This work was supported in part by the Nissan Science Foundation of Japan.

- 
- <sup>1</sup>For example, T. Ishiguro, K. Yamaji, and G. Saito, *Organic Superconductors*, 2nd ed. (Springer-Verlag, Berlin, 1998).
- <sup>2</sup>T. Mori, A. Kobayashi, Y. Sasaki, H. Kobayashi, G. Saito, and H. Inokuchi, *Bull. Chem. Soc. Jpn.* **57**, 627 (1984).
- <sup>3</sup>T. Mori, *Bull. Chem. Soc. Jpn.* **71**, 2509 (1998).
- <sup>4</sup>Y. Iwasa, K. Mizuhashi, T. Koda, Y. Tokura, and G. Saito, *Phys. Rev. B* **49**, 3580 (1994).
- <sup>5</sup>T. Hasegawa, K. Inukai, S. Kagoshima, T. Sugawara, T. Mochida, S. Sugiura, and Y. Iwasa, *Chem. Commun. (Cambridge)* **1997**, 1377 (1997).
- <sup>6</sup>T. Hasegawa, S. Kagoshima, T. Mochida, S. Sugiura, and Y. Iwasa, *Solid State Commun.* **103**, 489 (1997).
- <sup>7</sup>T. Mochida, T. Hasegawa, S. Kagoshima, S. Sugiura, and Y. Iwasa, *Synth. Met.* **86**, 1797 (1997).
- <sup>8</sup>R. Kondo, T. Hasegawa, T. Mochida, S. Kagoshima, and Y. Iwasa, *Chem. Lett.* **1999**, 333 (1999).
- <sup>9</sup>T. Hasegawa, T. Mochida, R. Kondo, S. Kagoshima, Y. Iwasa, T. Akutagawa, T. Nakamura, and G. Saito, *Phys. Rev. B* **62**, 10 059 (2000).
- <sup>10</sup>J. B. Torrance, J. E. Vazquez, J. J. Mayerle, and V. Y. Lee, *Phys. Rev. Lett.* **46**, 253 (1981).
- <sup>11</sup>R. M. Metzger and J. B. Torrance, *J. Am. Chem. Soc.* **107**, 117 (1985).
- <sup>12</sup>Y. Iwasa, T. Koda, Y. Tokura, A. Kobayashi, N. Iwasawa, and G. Saito, *Phys. Rev. B* **42**, 2374 (1990).
- <sup>13</sup>S. Aoki and T. Nakayama, *Phys. Rev. B* **56**, R2893 (1997).
- <sup>14</sup>A. Girlando, F. Marzola, C. Pecile, and J. B. Torrance, *J. Chem. Phys.* **79**, 1075 (1983).
- <sup>15</sup>Y. Tokura, H. Okamoto, T. Koda, T. Mitani, and G. Saito, *Solid State Commun.* **57**, 607 (1986).
- <sup>16</sup>M. Le Cointe, M. H. Lemeë-Cailleau, H. Cailleau, B. Toudic, L. Toupet, G. Heger, F. Moussa, P. Schweiss, K. H. Kraft, and N. Karl, *Phys. Rev. B* **51**, 3374 (1995).
- <sup>17</sup>A. Painelli and A. Girlando, *Phys. Rev. B* **37**, 5748 (1988).
- <sup>18</sup>T. Luty, *J. Chem. Phys.* **87**, 3137 (1987).
- <sup>19</sup>K. Murata, H. Yoshino, H. O. Yadav, Y. Honda, and N. Shirakawa, *Rev. Sci. Instrum.* **68**, 2840 (1997).
- <sup>20</sup>E. Demiralp and W. A. Goddard, *J. Phys. Chem. A* **102**, 2466 (1998).
- <sup>21</sup>A. Painelli and A. Girlando, *J. Chem. Phys.* **84**, 5655 (1986).
- <sup>22</sup>K. Takaoka, Y. Kaneko, H. Okamoto, Y. Tokura, T. Koda, T. Mitani, and G. Saito, *Phys. Rev. B* **36**, 3884 (1987).
- <sup>23</sup>Y. Tokura, T. Koda, T. Mitani, and G. Saito, *Solid State Commun.* **43**, 757 (1982).
- <sup>24</sup>J. S. Chappell, A. N. Bloch, W. A. Bryden, M. Maxfield, T. O. Poehler, and D. O. Cowan, *J. Am. Chem. Soc.* **103**, 2442 (1981).
- <sup>25</sup>H. Okamoto, T. Koda, Y. Tokura, T. Mitani, and G. Saito, *Phys. Rev. B* **39**, 10 693 (1989).
- <sup>26</sup>Thermal contraction effect of the pressure medium Daphne 7373 with decreasing of the temperature was investigated by Murata and co-workers (Ref. 19). The contraction is prominent above the frozen point of the medium located at around 200 K, which causes the additional resistivity anomalies in Fig. 5. (For example, such an anomaly is seen around 160 K at  $3 \times 10^4 \Omega \text{ cm}$  for the 0.24 GPa curve.) Below the frozen point, this effect is so small that we can neglect it in the temperature dependence of the resistivity. The applied pressure values were calibrated at the respective NI transition temperatures for each resistivity curves, to obtain the precise pressure-temperature phase diagram shown in Fig. 6.
- <sup>27</sup>T. Mitani, Y. Kaneko, S. Tanuma, Y. Tokura, T. Koda, and G. Saito, *Phys. Rev. B* **35**, 427 (1987).
- <sup>28</sup>N. Nagaosa and J. Takimoto, *J. Phys. Soc. Jpn.* **55**, 2745 (1986); N. Nagaosa, *ibid.* **55**, 3488 (1986).
- <sup>29</sup>M. H. Lemeë-Cailleau, M. Le Cointe, H. Cailleau, T. Luty, F. Moussa, J. Roos, D. Brinkmann, B. Toudic, C. Ayache, and N. Karl, *Phys. Rev. Lett.* **79**, 1690 (1997).
- <sup>30</sup>H. Okamoto, T. Mitani, Y. Tokura, S. Koshihara, T. Komatsu, Y. Iwasa, T. Koda, and G. Saito, *Phys. Rev. B* **43**, 8224 (1991).
- <sup>31</sup>S. Horiuchi, R. Kumai, Y. Okimoto, and Y. Tokura, *Phys. Rev. B* **59**, 11 267 (1999).
- <sup>32</sup>We calibrated pressure values for the phase diagram of (TTF)(CA) reported by Mitani *et al.* (Ref. 27).